Gemini Mauna Kea Laser Guide Star System

Céline d'Orgeville*, Mark R. Chun, Jacques Sebag, Corinne Boyer, David Montgomery, Jim M. Oschmann, François Rigaut, Doug A. Simons

Gemini Observatory, 670 N. A'Ohoku Place, Hilo, HI 96720

ABSTRACT

We discuss the design of the laser guide star system to be implemented with ALTAIR, the Gemini North adaptive optics system. We give an overview of the sodium physics in order to understand why some lasers are more efficient than others to produce bright artificial stars. We present some simulation results which set the laser output power requirement when launching a perfect beam to the sky. Preliminary designs for the beam transfer optics, the laser launch telescope and the safety systems are also presented.

Keywords: Sodium Laser Guide Star Adaptive Optics, sodium physics, LGS AO Strehl ratio

1. INTRODUCTION

The Gemini 8-m Telescopes Project is building two 8-m telescopes which will be equipped with Laser Guide Star Adaptive Optics (LGS AO). The Mauna Kea Telescope in Hawaii was dedicated in June 1999 and obtained its first astronomical images with the University of Hawaii adaptive optics system Hokupa'a, a natural guide star 36 actuators curvature system. Though operational handover will not happen before mid-2000, the images were close to the theoretical diffraction limit of an 8 meter telescope, achieving 80 milliarcsecond in K (2.2 microns). In 2001, Gemini North will be equipped with the first altitude-conjugated Shack-Hartmann adaptive optics system ever built for astronomy. This system, ALTAIR, will support both Natural Guide Star (NGS) and Laser Guide Star (LGS) observation modes[1]. At Cerro Pachon in Chile, the Gemini South telescope first light is expected during year 2000. This telescope will also eventually be equipped with laser guide star adaptive optics.

Both laser guide star systems at Mauna Kea and Cerro Pachon will use sodium beacons - as opposed to other schemes, either Rayleigh beacon or other atoms than sodium - for reasons which have been widely discussed in the past [2]. First, the adaptive optics system needs to use a light source located as far as possible from the telescope so as to reduce the cone effect. This is especially important when dealing with apertures as large as 8 meters. From this point of view, focusing a laser on the 90 km high, 10 km thick mesospheric sodium layer is preferred over using low-altitude Rayleigh scattering. Second, sodium seems to be the atomic species in the mesosphere which exhibits the best compromise between absorption cross-section and density. That is to say it is likely to emit the highest number of photons when excited by a 589 nm beacon in resonance with the sodium D2 line.

This paper intends to give an overview of the preliminary work that has been done at Gemini in order to design the future laser guide star system to be implemented on Mauna Kea. The first step was to understand the physics of sodium/light interaction as photon return does not depend only on laser power but also on temporal and spectral laser characteristics. The second step was to establish an error budget for the Mauna Kea LGS AO system and derive the requirements for the laser. Finally, the third step was to break the LGS system into subsystems and understand how each of them is to interact with the Gemini telescope. Future work includes the selection of a laser, completion of the final design and realization of the overall LGS system to use with ALTAIR.

2. THE PHYSICS OF SODIUM / LASER INTERACTION

Extensive work has been done by US Air Force and astronomers in order to understand how a ground based laser can excite mesospheric sodium atoms with the most efficient photon return to the ground based telescope. We will not produce any new result here since our purpose is rather to offer the reader a synthetic – though non-exhaustive – look at the issues related to the choice of a laser for LGS AO operation. We will instead refer to some of the many papers dealing with sodium / light interaction simulation and experiments that have been published during the past ten years.

---

* Correspondence: Email: cdorgeville@gemini.edu; WWW: http://www.gemini.edu; Telephone: (808) 974 2545

Sodium D2 line

The sodium atomic transition under interest in sodium laser guide star is the sodium D2 line around 589 nm. 589 nm photons produced by different laser formats, for example continuous wave (CW) or pulsed and longitudinally monomode or multimode, do not all interact with sodium atoms with the same efficiency. What we call efficiency here is the excited sodium atoms ability to emit 589 nm photons back towards the earth when decaying from their excited state, versus the averaged output power of the laser. Understanding how efficient the mesospheric sodium/laser light interaction will be for a given laser starts with having a closer look at the atomic sodium spectroscopy. References [3, 4, 5] give a detailed description of the sodium atomic levels and how one calculates them.

Basically, the sodium D2 line is made out of multiple possible transitions between the 8 atomic levels in ground state $3S_{1/2}$ and the 16 atomic level in the first excited state $3P_{3/2}$. Fig. 1 in ref. [4] shows the twenty-four magnetic substates and their relative energy levels. The $3S_{1/2}$ ground state is split into two hyperfine components 1.772 GHz apart. Hyperfine splitting inside the first excited state exhibits less contrast, so that all the atomic transitions are packed within two groups labeled according to the total angular momentum number F=1 or F=2 of the ground hyperfine substate (see fig. 3 (b) in ref. [3]). The radiative lifetime τ due to spontaneous emission of an atom in either of the excited states is 16 ns, which gives any two-level transition a natural linewidth of $1/(2\pi\tau)$ = 10 MHz. Doppler broadening due to the mesosphere temperature of about 200 K enlarges every individual transition line by 1.07 GHz. Fig. 2 in ref. [4] shows the resulting mesospheric sodium D2 line, with an overall profile of about 3 GHz full width at half maximum (FWHM). The sodium D2 line has two major peaks reflecting the ground state hyperfine splitting.

Saturation

There is a fundamental limitation to the amount of fluorescence photons a population of atoms can radiate when excited (i.e. pumped) by a resonant laser. Under strong continuous pumping, about half of the atoms are in the excited state whereas the other half are in the ground state. The situation does not change much by increasing the pump intensity because stimulated emission, which competes with fluorescence, gets stronger. The only photons useful for creating the artificial star are the ones inside the solid angle sustained by the telescope pupil. Atoms which decay due to stimulated emission emit photons in the forward direction and hence do not contribute to the brightness of the laser guide star. Ways to increase backward fluorescence photons are considered in the following sections.

CW laser

The highest photon returns for a 10 MHz linewidth CW laser are obtained when the laser frequency is locked on the F=2 → F=3 atomic transition, which corresponds to the peak of the D2 line. A two level approach drives a saturation intensity I_{sat} = 95 W/m^2 for single frequency excitation with a laser tuned at the peak and linearly polarized [7], and I_{sat} = 64 W/m^2 for the same laser when circularly polarized [3, 4, 6, 7]. The saturation power value is also linked to the LGS system ability to focus the laser beacon at the sodium layer. If the LGS system produces a 1 arcsec spot with uniform illumination of the sodium atoms, then the laser power to reach saturation is $P_{sat} = I_{sat} * \pi (\alpha H / 2)^2$ where α = 1 arcsec and H = 90 km. That is 14.2 W for a linearly polarized monomode 10 MHz CW laser and 9.6 W for the same laser with circular polarization. P_{sat} respectively drops down to 3.5 and 2.4 W when the spot size is 0.5 arcsec. Note that these numbers are valid for uniform illuminations. They change slightly for gaussian illuminations, because atoms in the gaussian core may be saturated whereas atoms in the aisles are not [4].

When saturation is reached with such a monomode laser, the power can be splitted between several velocity groups by using for instance a multimode laser or some phase modulation. The spectrum of an ideal laser would continuously fill the whole D2 line, allowing considerably higher saturation limits. No such ideal high power broadband CW laser is available today [8]. Existing LGS AO systems that are equipped with a narrow linewidth CW laser are not hit by saturation yet, because they are still limited by large spot sizes [9, 10, 11, 12].

Pulsed lasers

Due to low output powers CW LGS systems cannot achieve high photon returns. Thanks to possibly higher average output power levels, pulsed laser systems offer an alternative for LGS AO systems which need high photon return. But caution must be exercised when assessing the required power level for a pulsed system, as photon return depends strongly on the temporal and spectral laser format. Milonni *et al.* [4, 13] present qualitative and quantitative results on the sodium interaction with long, intermediate and short-duration pulses. Here a pulse is said to be long or short with comparison to the excited state lifetime of 16 ns. Because they have high peak powers, long pulses lead to saturation long before the end of the pulse duration, which makes them rather inefficient. Therefore long-pulse lasers reach saturation at relatively low average powers [14]. Note that in order to share saturation among all the velocity groups of mesospheric sodium atoms, those lasers must have a spectral profile close to the sodium D2 absorption line profile. On another hand, short pulse lasers with repetition rate higher than 1/(16 ns) = 62 MHz (typically, mode-locked lasers) provide a quasi-continuous excitation to the sodium atoms. Due to the

wide spectral format of such lasers (typically 1 GHz), a large number of velocity groups are excited. Therefore the eventual saturation is reached at higher average powers than, for instance, monomode CW lasers. For any practical use (P<200W) the photon return is linear with the laser average power [13, 15].

Optical pumping

In order to achieve high photon return, not only the laser temporal and spectral format matter but also its polarization. Linearly and circularly polarized light do not induce the same two-level transitions. Let us assume that a CW laser is tuned to the peak of the sodium D2 line and is circularly polarized (right polarization). After sufficiently long irradiation, atoms will be trapped in the F=2, m=2 → F=3, m=3 transition (see fig. 1 in ref. [4]). There is a strong interest in forcing all atoms to remain in that particular two-level transition. When atoms in the F=3, m=3 excited state decay, they can only emit circularly polarized photons. Such photons are preferentially emitted in the forward and backward directions. This leads to an additional 1.5 coefficient on the photon return. Optical pumping can be achieved by using circularly polarized lasers either CW or pulsed. However the pulse duration must be greater than about 20 optical cycles [3], that is 320 ns, for optical pumping to take place. Atomic collisions and the atoms' interaction with the earth magnetic field contribute to decrease the optical pumping efficiency, because they allow some atoms to decay down to the F=1 hyperfine ground state, 1.772 GHz away from the laser central frequency. To be fully efficient, the spectrum of such a laser should exhibit a second but less powerful line so that F=1 atoms get a chance to be pumped back into the F=2, m=2 → F=3, m=3 transition. Note that optical pumping into the F=2, m=-2 → F=3, m=-3 transition is also possible thanks to left-circular polarization.

Radiation pressure

In ref. [13, 15], Telle *et al*. propose the use of a 'slope efficiency' number to compare the efficiencies of various laser formats, all other parameters being equal (see table 2 and section 4). Surprisingly, it appears that a 10 MHz CW laser is less efficient than a macro-micro pulse laser of equal power. Note that both are below saturation. The cause is the radiation pressure effect. Because a macro-micro pulse laser has a wider spectrum, it can excite multiple velocity groups, whereas the monomode laser is locked on the zero velocity group only. Each time an atom absorbs one laser photon and re-radiate it in an arbitrary direction, its linear momentum is changed and its resonant frequency shifts. After a few optical cycles, the atom is literally pushed out of resonance because of radiation pressure, and optical pumping cannot take place. Because the atom jumped from its initial velocity group to the next, the single frequency CW laser cannot excite the atom any more whereas the macro-micro pulse laser does.

3. GEMINI MAUNA KEA LGS AO REQUIREMENTS

The main science driver for implementing LGS is to increase the number of science targets observable with ALTAIR. To this end, a bright sodium laser guide star is necessary with as small a size as possible. In order to establish a required LGS brightness and shape/size, we readdressed the original 'high-priority' science cases for the Gemini AO. Morris *et al*.[1] find that while there are compelling cases for a high Strehl (S~0.5 @ 1.65 microns), these cases (brown dwarfs, young stellar objects, and planet searches) generally act as their own wavefront reference. Namely, these scientific cases do not drive the need for a laser guide star. On the other hand, the science cases which drive the laser guide star requirement, for example spectra of high redshift field galaxies, are enabled by a more moderate Strehl of 0.2-0.3.

The minimum Strehl for the ALTAIR+LGS system strongly drives the specification of the laser because the laser technology is still developing and the focal-anisoplanatism is so large. Our basic requirement is to match the science objectives of ALTAIR. As such, the goal for the telescope + LGS AO system is a Strehl ratio greater than 0.2 in H-band during median conditions in the focal-plane of the science instrument. To compare this with the simulations, we note that the uncorrected telescope and instrument aberrations alone lead to a Strehl degradation of approximately 64% [16]. This places a Strehl requirement of 0.31 on the residual atmosphere aberrations after the LGS AO combination under our median conditions. The median conditions, also used in the simulations, are conservatively chosen so that the MK LGS AO system meets its specifications during all but the worse conditions. Nominal conditions are as follows:

- 45 degrees zenith angle
- Median-to-Poor seeing conditions at Mauna Kea: r0=17.2 cm @ 589 nm (equivalent to 0.7 arcsec seeing @ 0.55 microns)
- Average/low sodium column density: $C_S=2*10^9$ atoms/cm^2
- Sodium layer altitude: H = 90 km (above sea level)
- Sodium layer thickness = 10 km (approximated as a gaussian, 1/e^2 diameter)
- Atmospheric transmission coefficient = 0.8 (one way)

The expected performance of ALTAIR when used with the LGS was calculated using an adaptive optics system simulation package written in IDL by one of us (F. R.). The principal features of this package are:
(1) Multiple layered phase screen turbulence (up to 5 screens)
(2) Temporal evolution of the turbulence (screen translation with a "frozen" turbulence)
(3) Wavefront sensing simulation including a fully diffractive formation of spots in a Shack-Hartmann wavefront sensor
(4) Deformable mirror hysteresis and influence functions
(5) Laser launched from the center or from the side of the telescope
(6) Propagation of the LGS beam upward and downward through atmosphere
(7) Inclusion of the focal-anisoplanatism by propagating the size of the phase screen 'illumination' through altitude
(8) Inclusion of the spot elongation (geometric)

The number of adjustable parameters in the simulations is extremely large. To minimize the latter we first chose a baseline set of parameters. Some parameters were fixed while others were individually optimized. The baseline set of conditions and the final optimized parameters are outlined in table 1. The optimized parameters were in order: the laser launch telescope tip/tilt gain, the AO loop gain, and the integration time. We also ran two simulations using the optimized parameters to compare Strehl ratio results when launching either from the center or from the side of the telescope. For a 9 magnitude star, the Strehl was 0.34 when launching from the center of the telescope but only 0.26 when launching from the side. Therefore, in order for the MK LGS AO system to meet its Strehl specification of 0.31, the only possible choice is to launch from the center of the telescope. With these parameters optimized, we then explored how the laser guide star magnitude and the seeing affected the Strehl. Fig. 1 presents the results for poor to median, good and excellent seeing conditions above Mauna Kea. On the poor to median seeing curve, the MK LGS AO Strehl requirement of 0.31 corresponds to a star magnitude of 11.6. This point stands on the falling part of the curve. We choose an 11 magnitude star, closer to the edge of the plateau to calculate the corresponding laser power requirement.

Parameters	**Baseline setting**	**Optimized values**
Number of actuators Number of subpupils	13*13 12*12	
WFS wavelength WFS read noise WFS pixel size	0.589 microns 4.5 e^-/pixel 0.95"/pixel	
Laser launch telescope position Laser launch telescope diameter Laser Beam $1/e^2$ diameter Laser tip/tilt mirror gain	Central (behind secondary) 0.45 m 0.30 m 0.1	Central (behind secondary) 0.5
AO loop gain AO integration time (one frame pure delay in control loop) Imaging wavelength	0.5 2 ms 1.6 microns	0.4 1.2 ms
r_0 @ 0.589 microns Number of turbulent layers	17.2 cm 5	

Table 1: Baseline LGS AO simulation parameters and optimized values

This simulation provides insight into the trade-offs in designing the LGS however it does not include telescope and focal-plane instrumentation aberrations (dynamic and static) and does not simulate the conjugation-to-altitude nature of ALTAIR. These two effects are important and the magnitude of their effect is estimated here. The telescope and instrument image quality error budgets were taken from the Gemini System Error Budget Plan by J. Oschmann [16]. The telescope residual errors include higher-order static optical errors in the primary and secondary mirrors, the AO fold mirror (the tertiary element), and the final science fold mirror. The instrument residual errors include any optical aberration within the science instrument which can not be deduced and corrected with static offsets within the AO system. Oschmann [16] estimates these contributions to have a Strehl degradation at 1.6 microns of 0.64. Ellerbroek and Tyler [17] have calculated the advantage of altitude conjugation with a sodium laser guide star. Under their nominal seeing conditions (which assume slightly better conditions than in this work), the on-axis Strehl performance is increased by roughly 10% at 1.65 microns. For the remainder of this work, the increase due to ALTAIR's conjugation to altitude was neglected.

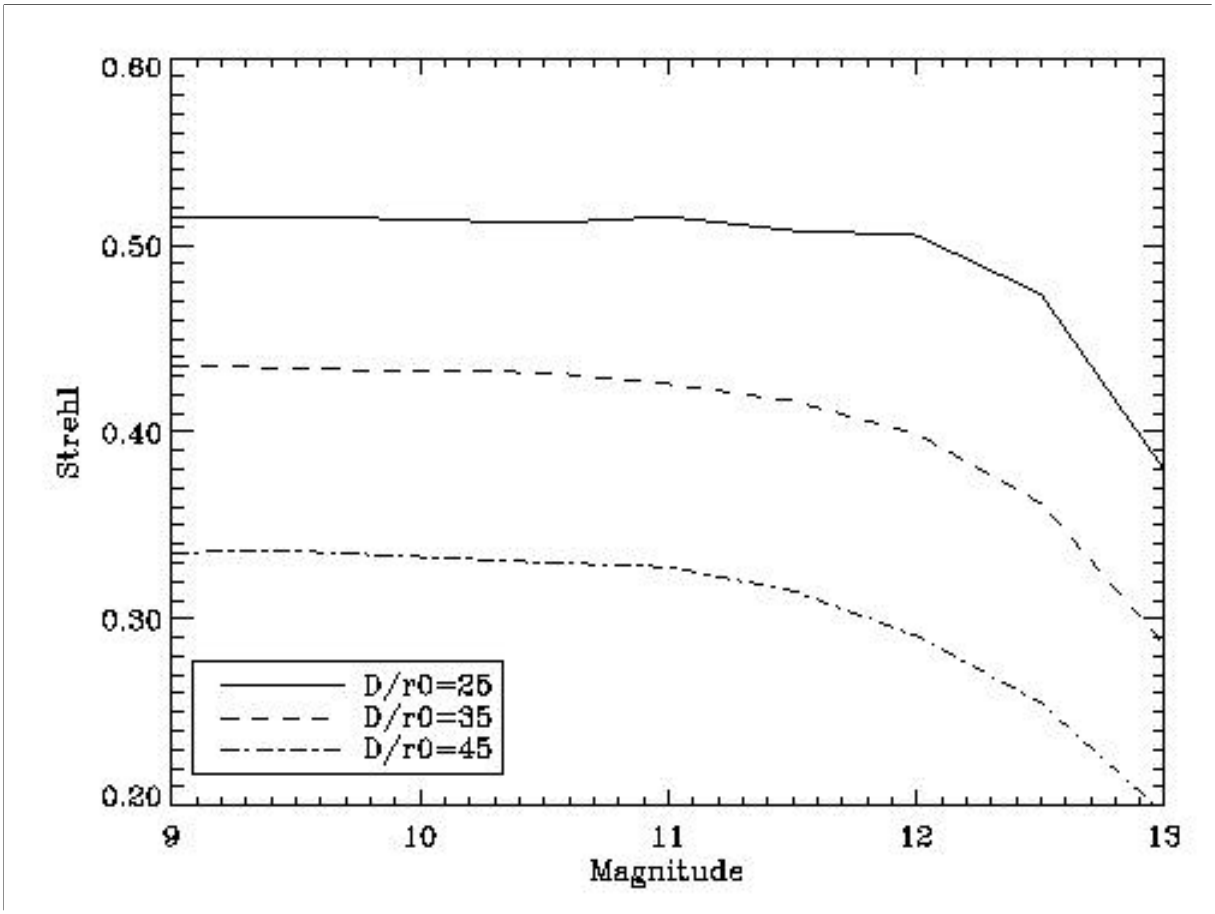

Fig. 1: Strehl ratio versus LGS magnitude for three different seeing conditions @ 589 nm. Dashed-dotted curve: r0 = 17.5 cm (poor to median); dashed curve: r0 = 22.6 cm (good); plain curve: r0 = 31.6 cm (excellent)

4. GEMINI MAUNA KEA LGS AO SUBSYSTEMS

The Mauna Kea laser guide star system (MK LGS) will be part of the Gemini North facility. As a facility instrument, it will be fully automated so that minimum set up work is required prior to observation mode, and high reliability is achieved through operation. The MK LGS system will be implemented and integrated on the telescope by the Gemini Adaptive Optics group. The overall MK LGS system consists of six identified subsystems: Laser System (LS), Laser Enclosure (LE), Beam Transfer Optics (BTO), Laser Launch Telescope (LLT), LGS Control System (LGS CS), and Safe Aircraft Localization and Satellite Acquisition System (SALSA). All subsystems but the laser will be developed in-house. The laser system requirements are derived from the MK LGS error budget. The relevant parameters addressed by the error budget are the photon return and the laser spot shape obtained after the laser light is propagated through the overall system plus the atmosphere, to the sodium layer.

The photon return calculation takes into account the following parameters: a) LS: detailed spectral format, tuning stability, temporal format, polarization, output power fluctuations b) BTO: number of optical elements and their transmission/reflection coefficient c) LLT: same as BTO, plus laser beam $1/e^2$ diameter d) Atmosphere: transmission coefficient @ 589 nm, sodium column density, sodium layer altitude and thickness.

The laser spot shape calculation takes into account some other characteristics of the same subsystems: a) LS: laser beam quality, beam pointing jitter b) BTO: laser beam $1/e^2$ diameter, Fried parameter equivalent to the atmospheric turbulence generated along the BTO path, number of optical elements and the aberrations they add to the laser wavefront, alignment, beam pointing stability, scattered light detected by the AO wavefront sensor c) LLT: same as BTO, without atmospheric turbulence d) Atmosphere: laser beam $1/e^2$ diameter at LLT pupil, and atmospheric seeing @ 589 nm.

As ALTAIR sampling frequency will be close to 1 kHz, we only consider every noise source on a 1 ms time scale. This means that atmospheric tip-tilt jitter (for instance) will have almost no blurring effect on the laser spot at the sodium layer.

Telescope flexures and pointing servo-loop errors will not have any influence either because they occur at frequencies lower than 1 kHz.

Laser System

Once we know the photon return and spot size requirements for the MK LGS AO system, we need to express them in terms of laser power and beam quality. Telle *et al.*[13, 15] propose the use of a 'slope efficiency' number to compare different laser format efficiencies. If saturation effects are small, the guidestar flux at the telescope primary mirror can be expressed in photons/cm^2/ms as:

$$N = SE \times (C_s \sec\theta) \times (T^{\sec\theta})^2 \times P \;/\; (H \sec\theta)^2$$

where SE is the non-saturated slope efficiency in photon-m^2/ms/watt/atom, C_s is the column density in atoms/cm^2, T is the atmospheric transmission from ground to the mesosphere for a zenith angle equal to 0 deg., P is the average laser power in watts immediately after the laser launch optics, H is the altitude of the sodium layer in meters, and θ is the zenith angle in degrees. In order to derive the laser power requirement, we assume θ = 45 deg., $C_s = 2*10^9$ atoms/cm^2, H = 90 km, T = 0.8. Besides, we assume w_0 = 15 cm for the gaussian beam waist (1/e2 radius) at the LLT pupil. This waist size is expected to be close to the optimum in median to poor seeing conditions (r0 = 17,2 cm @ 589 nm) when projecting the gaussian beam from a 45 cm LLT [18]. The power loss by aperture clipping of the gaussian beam equals $1 - \exp(-2a^2/w^2)$ where a is the aperture radius and w is the 1/e^2 beam radius [19]. Together with the optical transmission of the LLT equal to 0.9, this gives an overall transmission coefficient $T_{LLT} = 0.9*0.99 \tilde{} \; 0.9$. To calculate the laser power which corresponds to a given star magnitude, we first calculate the photon flux at the ground. We assume a quantum efficiency of 0.85 for the detector and an optical throughput of 0.7 for the AO optics in the visible and 0.7 for the telescope + the AO fold mirror, so that the global telescope + AO optics + detector is $T_{global} = 0.42$. Then the photon flux at the ground (these are the photons received by the telescope pupil) is, in photons/cm^2/s:

$$N = \frac{4.10^{11}}{S * T_{global}} 10^{-\frac{m_V}{2.5}}$$

where m_V is the star magnitude and S = 4.8 10^5 cm^2 is the telescope pupil area. From these two equations we deduce the laser power P launched to the sky and we finally calculate the laser output power:

$$P_{output} = \frac{P}{T_{BTO}.T_{LLT}}$$

Table 2 presents the power requirements for three laser formats in terms of power at the output of the laser (optics and atmosphere are included) for a 11 and 11.6 magnitude star. Fig. 2 shows how the Strehl ratio is expected to evolve with increasing laser output power for an ideal beam launched at the sky.

Laser format	CW laser Monomode FWHM=10 MHz Circular polarization		Long pulse laser 100 ns pulse @ 30 kHz rep. rate Phase modulated FWHM=3 GHz Any polarization		Macro-micro pulse laser 150 μs @ 400 Hz rep. rate 700 ps @ 100 MHz rep. rate Mode-locked FWHM=1 GHz Circular polarization	
Slope efficiency (photon-m^2/ms/watt/atom)	0.26 ±10 %		0.10 ±10 %		0.33 ±20 %	
T_{BTO}	0.6		0.8		0.8	
LGS magnitude (V band)	11.6	11	11.6	11	11.6	11
Photon flux (ph./cm^2/s)	46	79	46	79	46	79
Laser output power (W)	3.5	**6.1**	6.8	**11.9**	2.1	**3.6**

Table 2: The three laser formats are close to real laser formats. The CW laser could be a Coherent 899-21 ring dye laser [10], the long pulse laser a pulsed dye laser such as the Lick or Keck lasers built by the Lawrence Livermore national Laboratory [20] and the macro-micro pulse laser the University of Chicago sum-frequency laser built by the Lincoln Laboratory [21]. The slope efficiency numbers are either given in ref. [13, 15] or assessed from the slope efficiencies of similar lasers. Note that the BTO transmission coefficient is different for the CW laser because this particular laser would have to be mounted further away from the telescope.

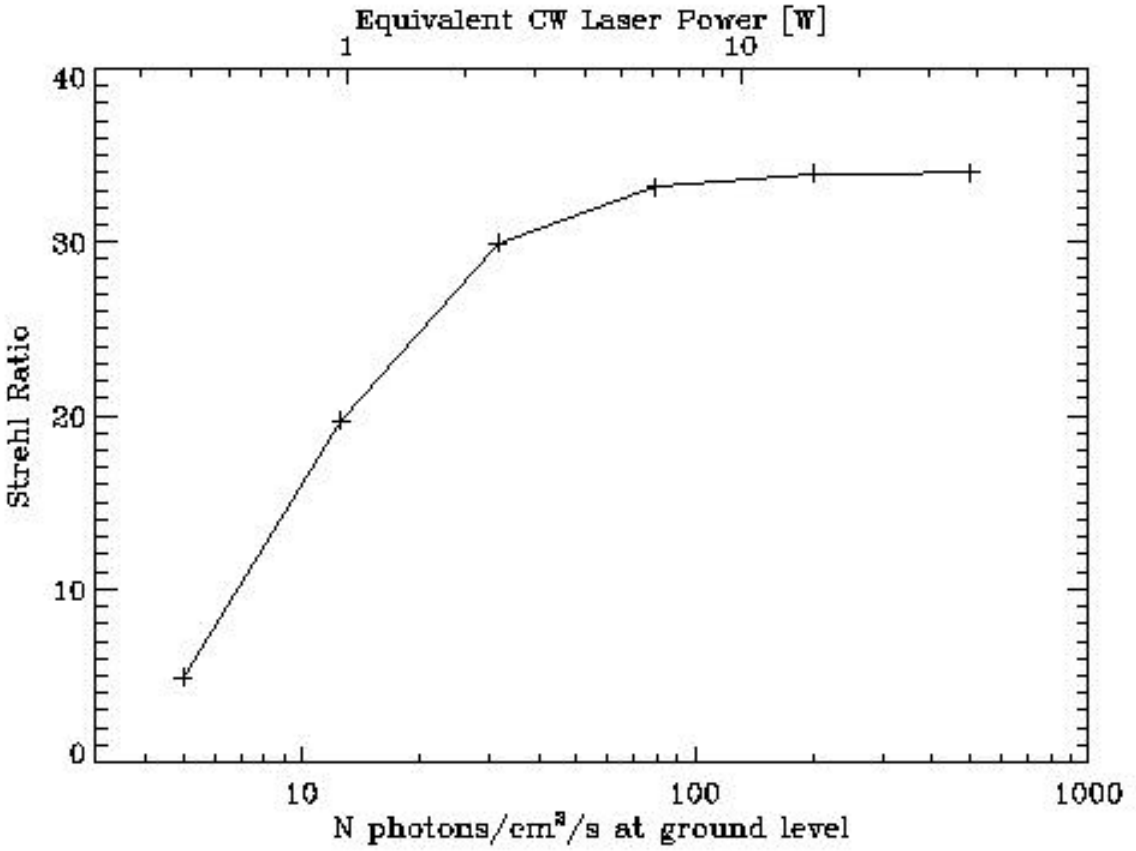

Fig. 2: Strehl ratio versus photon flux at the ground and laser output power (monomode 10 MHz CW laser). Equivalent output powers for other laser formats can be deduced by using the 'slope efficiency' numbers and the adequate transmission coefficients for a similar LGS AO system.

Up to now, the laser beam quality has not been taken into account in the simulations yet, and we expect the laser power requirement to be driven up by the use of a non-ideal gaussian beam. Note that atmospheric turbulence effects and geometric elongation of the laser spots were included though. Telle *et al.*[15] give a simplified formula to assess the spot FWHM at the sodium layer:

$$\sqrt{\left(\left(\frac{l}{r_0}\right)^2+\left(\mathrm{DL}\left(\frac{l}{2a}\right)\right)^2\right)}$$

where DL is the laser beam quality in terms of the number of times diffraction limited. Let us assume that we use a beam 1.1 times diffraction limited. With r_0 = 17.2 cm and 2a = 45 cm the LGS system would then produce a 0.77 arcsec spot at the sky. We intend to run some simulations with the General Laser Analysis and Design software (GLAD) from Applied Optics Research to understand how a non ideal gaussian beam plus some random aberrations due to poor optical surfaces, optics aberrations, dust scattering or LLT misalignment can alter the spot shape at the sky. The furthest subpupils are more than likely too small to enable the centroiding of blurred spots. Therefore we will have to increase and optimize the increased pixel size too. Noise will increase as a drawback, driving the need for higher photon returns. That is the reason why we intend to run our AO code again to derive more realistic output power and beam quality requirements for the laser system.
The laser location is another great concern for the laser system. As a matter of fact, the shorter the BTO path, the less power loss and the best beam quality we get for the laser beam at the LLT. Reasons of symmetry and reasonable laser output power lead to launch the laser beam from behind the secondary mirror of the telescope. No laser can be mounted on the telescope top-end, but several laser locations have been investigated either on the telescope center section, on the telescope access platform or even further in the pier below the telescope (see fig. 3). Issues with each of those locations are, in order,

vibrations, heat removal, cooling, power supply and access for maintenance. The best location would be on the center section (location A in fig. 3), but in that case the laser output power and its wavelength must keep stable under gravity change.

Beam Transfer Optics

The beam transfer optics (BTO) are the components needed to bring the beam from the output of the laser system to the input of the laser launch telescope. The positioning of the LGS on the sky is controlled by this subsystem. The system includes active control of the beam direction and supply diagnostics on the beam pointing (far- and near-field), an indication of the beam quality, and the beam power. The BTO design is strongly dependent on the laser location. The nominal design consists in a train of high quality, high reflectivity dielectric mirrors optimized for 589 nm, plus a relay telescope to control the beam size on the laser launch telescope. If the laser is located on the center section (location A in fig. 3) this would be 6 to 7 mirrors. But if for any reason the laser has to be located further away, for instance in the pier under the telescope (location B in fig. 3), then the number of mirrors could increase up to 15. The laser beam could be directed to the top-end from a point located on the elevation axis, in front of the elevation bearing. Or it could be propagated along the elevation axis, through the elevation bearing, to the center section and from there directed to the top-end. We have also investigated the possibility to propagate the beam through optical fibers [22], but such a design would require some development work. There are three major difficulties. The first one is to increase the coupling efficiency of the laser beam into the fiber. The second one is to overcome Brillouin scattering in the fiber. This non-linear effect increases with the laser intensity in the fiber core and decreases with the laser spectrum width (smaller linewidths create more Brillouin scattering). Finally the third difficulty is to match the output beam f ratio with the laser launch telescope optics. Fibers offer an elegant solution for the BTO design, but their overall transmission coefficient is always sensibly lower than the transmission coefficient of an all-mirror design.

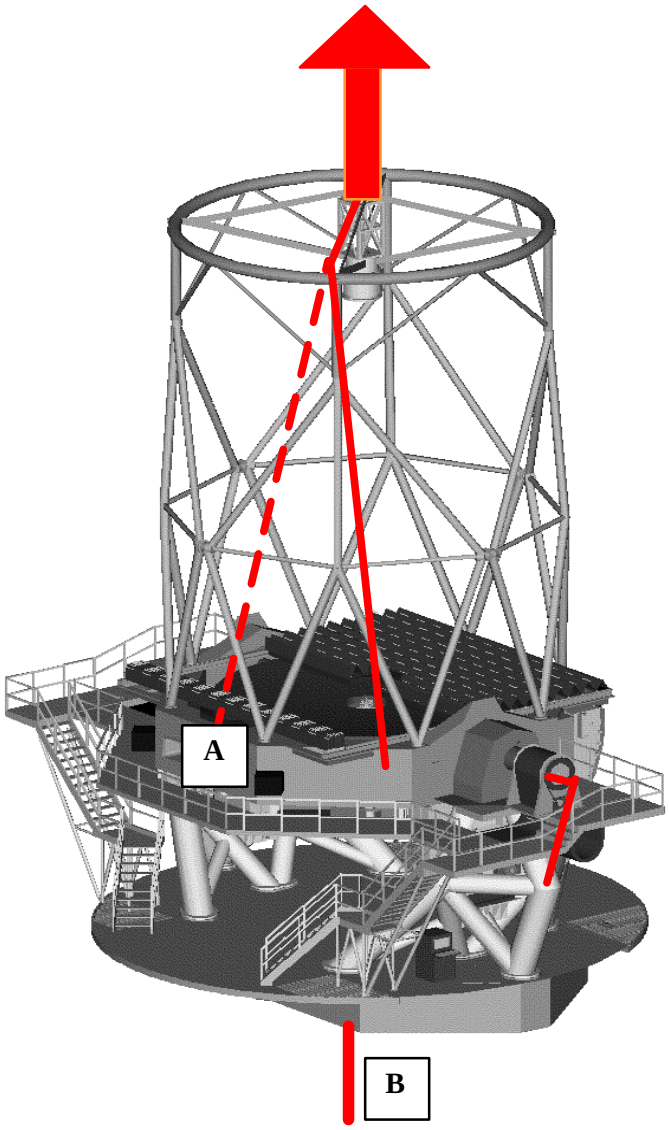

Fig. 3: Two possible laser locations and the laser beam path to the laser launch telescope. Location A is on the side of the telescope center section. Location B is in the pier under the telescope.

Laser Launch Telescope

Two main configurations are available for designing the laser launch telescope (LLT): it could be off-axis attached to the side of the main telescope, or on-axis mounted behind the secondary mirror. Gemini has chosen the on-axis configuration because although it requires a more careful implementation, it minimizes the laser power and facilitates the LGS wavefront sensing. The LLT will be inserted inside the secondary central frame of the Gemini telescope. This structure holds the secondary mirror and positioning system on one end, and is attached to the top end ring through eight thin vanes (see fig. 4). There are some constraints related to that configuration. For example, getting the laser beam behind the secondary requires hiding the beam in the shadow of the top end vanes. Also, the secondary frame and the top end have to be designed to accept and to support this weight. Thanks to an early choice, these aspects were taken into consideration when designing the telescope. For example, some space has been kept to insert the LLT inside the central frame, and extra weights are now mounted on the telescope for balancing purpose to be removed once the LLT is in place. Because Gemini is infrared

oriented, the LLT should not block the secondary central hole when not in use. This leads to design a retractable LLT primary mirror to be able to park it away. As shown on fig. 5 this move could be done with an actuator positioned inside the LLT. This actuator would be used only at the beginning or at the end of the night to position the mirror. This additional heat source above the secondary will not be a problem for observing.

Fig. 4: Secondary mirror central frame

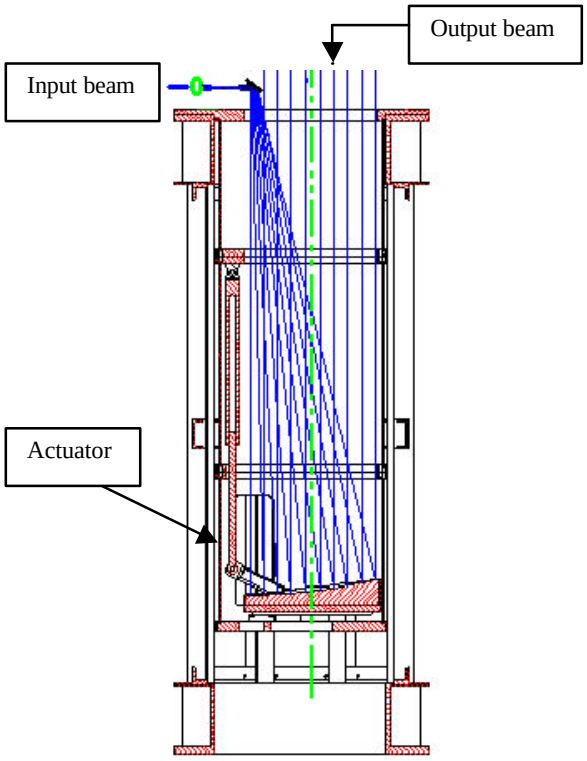

Fig. 5: Retractable mirror scheme

Optically, the LLT is equivalent to a laser beam expander. It receives a collimated laser beam with a small diameter, magnifies it and points it to the sky. The main requirements for Gemini are an output diameter of 450 mm, a magnification close to 100 and a field of view of ±1 arcmin. Different designs are currently being investigated. The element they have in common is an off-axis parabolic primary mirror. This choice allows the laser beam to enter from the top of the central frame without vignetting the output beam (see fig. 6). The plan is to use a standard off-axis parabolic mirror in order to limit the cost. Then, the secondary "mirror" is adapted to the characteristics of the off-axis. It could be a reflective or refractive element. In fig. 6 we studied a reflective/refractive combination. This configuration is equivalent to a Keplerian beam expander, and has the advantage of having an internal focus position that could be used as a reference for the beam transfer optics or to position a shutter.

To simplify the integration of the system, the LLT is envisioned as a standalone instrument mounted in its own structure with specific interfaces to the secondary frame. This allows for the unit to be tested and aligned before mounting on the telescope. Special care has to be taken for the integration inside the telescope where the space between the dome and the central frame is very limited. In the time coming, we need to do a more detailed opto-mechanical study of this system before we choose a final configuration.

Safety Systems

The Safe Aircraft Localization and Satellite Acquisition system (SALSA) includes all components internal to the observatory needed to prevent illuminating an airplane or satellite. Aircraft will be detected using a camera (visible or IR) which covers a narrow (5-10 degree) field of view along the laser propagation axis. Any object moving in the field will signal the LGS-Control System to open-loop ALTAIR and shutter the laser. This system complements the Laser Traffic Control System mountain-wide aircraft detection cameras. Currently, to avoid damage to earth-orbiting satellites, the propagation of lasers with peak optical powers greater than 3 Watts must be coordinated with Space Command. A close look at the American National Standard for Safe Use of Lasers [23] shows that the 3 W limitation corresponds in our case to a factor of two lower

than the Maximum Permissible Exposure (MPE) for an aircraft pilot who would fly through the gaussian beam peak intensity at 200 km/h speed. Such a laser could be propagated safely into the sky.

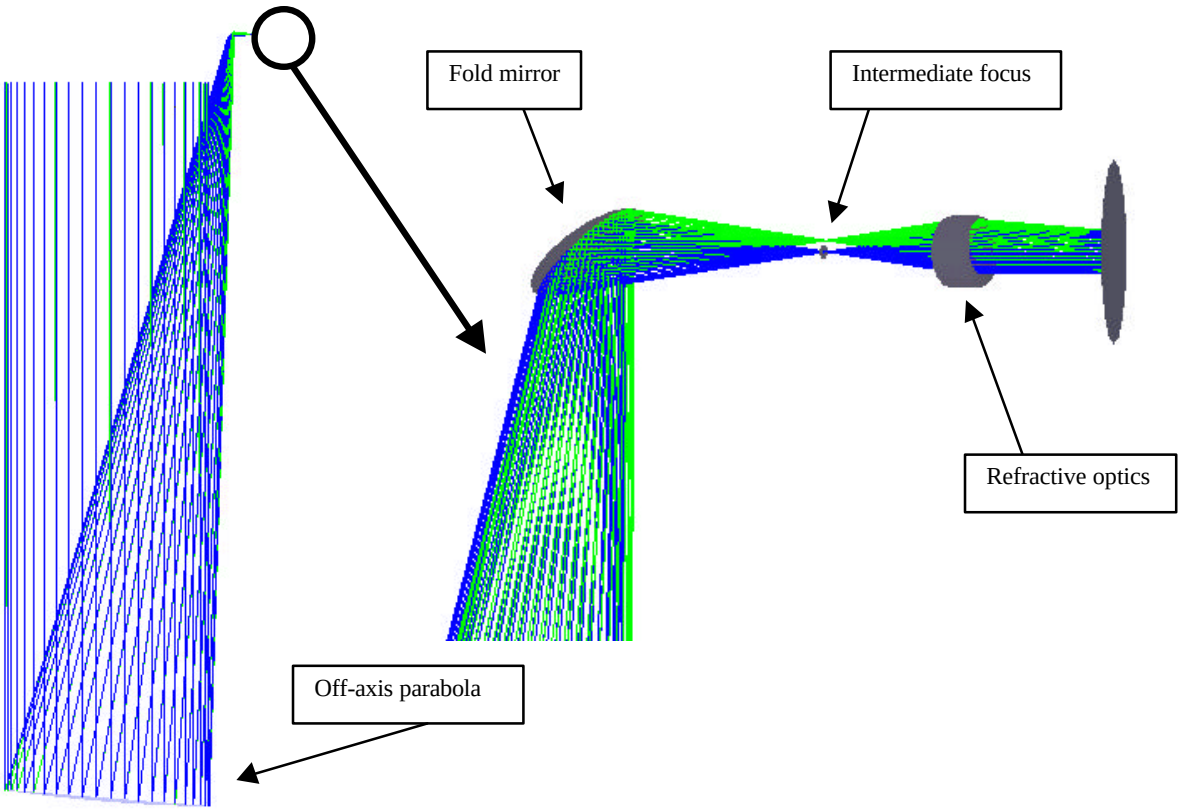

Fig. 6: Laser launch telescope optical design

5. CONCLUSION

The physics of sodium/light interaction is now well understood, as well as the different efficiencies for existing laser formats. However no ideal laser to use for sodium laser guide star adaptive optics is readily available nowadays. In order to write the laser requirements for the Mauna Kea laser guide star adaptive optics system, we simulated the Strehl ratio of an image compensated by the MK LGS AO in the instrument focal plane. A non-aberrated laser which creates a 11 magnitude guide star meets our Strehl requirement of 0.31. The equivalent output powers for a continuous wave monomode laser, a long pulse and a macro-micro pulse laser are respectively 6.1 W, 11.9 W and 3.6 W. The power requirements are however expected to be driven up by taking into account the real beam quality of the laser at the laser launch telescope.

Besides the photon return and corresponding laser power requirements for the Mauna Kea laser guide star system, some preliminary considerations and early designs have been presented for the beam transfer optics, the laser launch telescope and the safety systems which are other subsystems of the LGS AO system. The beam transfer optics design mostly depends on the laser location, whereas the laser launch telescope is an almost independent entity. Launching the laser beam from behind the secondary mirror, as opposed to the side of the telescope, is an absolute requirement for the Gemini North LGS system.

6. ACKNOWLEDGMENTS

The authors wish to thank deeply the participants to the Adaptive Optics Working Group forums held in Hilo, Dec. 10-11, 1998 and April 19-20 1999, for their invaluable input on laser guide star and adaptive optics technologies.

7. REFERENCES

1. S. Morris, G. Herriot , T. Davidge, "Gemini Adaptive Optics System Operational Concepts Definitions Document Rev. D", 1997
2. I. A. De La Rue and B. L. Ellerbroeck, "A study of multiple guide stars to improve the performance of laser guide star adaptive optical systems", *SPIE Proceedings*, vol. 3353, pp. 310-319, 1998
3. Thomas H. Jeys, "Development of a mesospheric sodium laser beacon for atmospheric adaptive optics", *The Lincoln Laboratory Journal*, vol. 4, No. 2, 1991
4. Peter Milonni, Robert Q. Fugate, and John M. Telle, "Analysis of measured photon returns from sodium beacons", *J. Opt. Soc. Am. A*, vol. 15, No. 1, Jan. 1998
5. Laurent Michaille, "Photon flux of the sodium LGS", *Imperial College private communication*, 1999
6. D. Hils, W. Jitschin, and H. Kleinpoppen, "Production of a highly polarized atomic beam", *Appl. Phys*., 25, pp. 39-47, 1981
7. Edward Kibblewhite, "The physics of sodium / laser interaction", presentation given at the Gemini AO working group, Hilo, HI, 10-11 Dec. 1998
8. Céline d'Orgeville, Daniel Muller, Alexandr Kachanov, Jean-Paul Pique, "A modeless laser for the Polychromatic Laser Guide Star Project", in preparation
9. A. Quirrenbach, W. Hackenberg, H.-C. Holstenberg, and N. Wilnhammer, "The sodium laser guide star system of ALFA", in *Adaptive Optics and applications*, SPIE Proceedings vol. 3126, 1997
10. A. Quirrenbach, W. Hackenberg, H.-C. Holstenberg, and N. Wilnhammer, "The ALFA dye laser system", in *ESO workshop on laser technology for laser guide star adaptive optics astronomy*, *ESO Proceedings*, vol. 55, pp. 126-130, 1997
11. Bruce P. Jacobsen, Ty Martinez, J. Roger P. Angel, Michael Lloyd-Hart, Steve benda, Dave Middleton, Herb Friedman, and Gaylen Herbert, "Field evaluation of two new continuous-wave dye laser systems optimized for sodium beacon excitation", *SPIE Proceedings*, vol. 2201, pp. 342-351, 1994
12. W. T. Roberts, Jr., T. Martinez, and J. R. P. Angel, "Sodium laser guide star used at the MMT", in *ESO workshop on laser technology for laser guide star adaptive optics astronomy*, *ESO Proceedings*, vol. 55, pp.86-91 1997
13. John M. Telle, Peter W. Milonni, and Paul D. Hillman, "Comparison of pump-laser characteristics for producing a mesospheric sodium guidestar for adaptive optical systems on large-aperture telescopes", in *High-power lasers*, *SPIE Proceedings* vol. 3264, 1998
14. K. Avicola, J. M. Brase, J. R. Morris, H. D. Bissinger, J. M. Duff, H. W. Friedman, D. T. Gavel, C. E. Max, S. S. olivier, R. W. Presta, D. A. Rapp, J. T. Salmon, and K. E. Waltjen, "Sodium-layer guide-star experimental results", *J. Opt. Soc. Am. A* 11, pp. 825-831, 1994
15. John M. Telle, Peter W. Milonni, Paul D. Hillman, and Robert Q. Fugate, "Laser requirements for pumping mesospheric sodium guidestars for adaptive optical systems on large aperture telescopes", to be published
16. Jim Oschmann, "Gemini System Error Budget Plan", *Gemini Project Document* SPE-S-G0041, 1997
17. B. Ellerbroek, and D. W. Tyler, "Adaptive optics sky coverage calculations for the Gemini-North Telescope", *PASP*, 110 (744), pp. 165-187, 1998
18. Bruce P. Jacobsen, "Sodium guide star projection for adaptive optics", Ph.D. thesis, University of Arizona, 1997
19. Anthony E. Siegman, "Lasers", p. 666, University Science Book, 1986
20. H. W. Friedman, G. V. Erbert, T. Kuklo, G. R. Thompson, N. J. Wong, D. T. Gavel, J. T. Salmon, and M. Feldman, "Design of a laser guide star system for the Keck II telescope", in *ESO workshop on laser technology for laser guide star adaptive optics astronomy*, *ESO Proceedings*, vol. 55, pp.138-151, 1997
21. Edward J. Kibblewhite and Fang Shi, "Design and field tests of an 8 watt sum-frequency laser for adaptive optics", *SPIE Proceedings*, vol. 3353, pp. 300-309, 1998
22. Domenico Bonaccini and Wolfgang Hackenberg, *ESO private communication*, 1999
23. "American National Standard for Safe Use of Lasers", ANSI Z136.1-1993